ELSEVIER

Journal of Alloys and Compounds 464 (2008) 101–106

Journal of ALLOYS AND COMPOUNDS

www.elsevier.com/locate/jallcom

Al-rich region of Al–Pd–Ru at 1000 to 1100 °C

D. Pavlyuchkov [a,b,*], B. Grushko [a], T.Ya. Velikanova [b]

[a] *Institut für Festkörperforschung, Forschungszentrum Jülich, D-52425 Jülich, Germany*
[b] *I.N. Frantsevich Institute for Problems of Materials Science, 03680 Kiev 142, Ukraine*

Received 5 July 2007; received in revised form 24 September 2007; accepted 24 September 2007
Available online 29 September 2007

Abstract

Partial isothermal sections of the Al–Pd–Ru phase diagram at 1000, 1050 and 1100 °C are presented here. The Al–Pd orthorhombic ε-phases dissolve up to ~15.5 at.% Ru, $Al_{13}Ru_4$ <2.5 at.% Pd and Al_2Ru up to 1 at.% Pd. Between 66 and 75 at.% Al, ternary quasiperiodic icosahedral phase and three cubic phases: C ($Pm\bar{3}$, $a = 0.7757$ nm), C_1 ($Im\bar{3}$, $a = 1.5532$ nm) and C_2 ($Fm\bar{3}$, $a = 1.5566$ nm) were revealed. An additional complex cubic structure with $a \approx 3.96$ nm was found to be formed at compositions close to those of the icosahedral phase.

Keywords: Intermetallics; X-ray diffraction; Phase diagram

1. Introduction

Al–Pd–Ru belongs to a group of alloy systems that exhibit the formation of quasicrystals and related complex periodic intermetallics [1]. According to the position of Ru in the periodic table, this alloy system is linked to the recently studied Al–Pd–Fe [2,3], Al–Pd–Rh [4] and Al–Ni–Ru [5].

The literature data on the Al–Pd–Ru alloy system are poor and limited to information on several individual phases. The formation of a cubic phase ($P23$; $a = 1.5540$ nm) was previously reported in this alloy system at $Al_{68}Pd_{20}Ru_{12}$ [6]. Another cubic phase ($Fm\bar{3}$; $a = 1.56058$ nm) was revealed at $Al_{66.8}Pd_{21.2}Ru_{12.0}$ [7] and one more (so-called (2/1) approximant with $a = 2.0$ nm) around $Al_{71}Pd_{19}Ru_{10}$ [8]. An icosahedral (I) quasicrystalline phase was found to be stable in the alloy $Al_{72}Pd_{17}Ru_{11}$ [9].

In the present contribution we report the preliminary investigation of the phases and phase equilibrium in Al–Pd–Ru in the Al–AlPd–Al_2Ru compositional triangle and temperature range of 1000–1100 °C. The boundary Al–Pd phase diagram is accepted according to [10] and Al–Ru according to [11].

2. Experimental

Sixty alloys were produced from the constituent elements by levitation induction melting in a water-cooled copper crucible under an Ar atmosphere. The purity of Al was 99.999%, of Pd 99.95% and of Ru 99.9%. Considering the high price of the components the ingots were typically of about 3 g. The dissolution of Ru in Al is difficult. Therefore, more homogeneous alloys were prepared using Ru powder which was first mechanically compressed with Pd powder into pellets and then melted together with Al. In addition, due to high-temperature peritectic formation of the phases in Al-Ru and ternary compositions, significant segregation occurred during solidification. Final ingots were quite inhomogeneous.

Parts of the samples were annealed under an Ar atmosphere or vacuum for different times depending on the annealing temperature. The annealing time at 1000 °C was up to 165 h, at 1050 °C up to 160 h and at 1100 °C up to 50 h.

Single-phase samples were selected using powder X-ray diffraction (XRD) and scanning electron microscopy (SEM). Their compositions were examined by inductively coupled plasma optical emission spectroscopy (ICP-OES) and by energy-dispersive X-ray analysis (EDX) in SEM. Powder XRD was carried out in the transmission mode using Cu K_1 radiation and a position-sensitive detector. The samples were also studied by electron diffraction in the transmission electron microscopes (TEM) JEOL FX 4000 and Philips CM 200 operated at 400 and 200 kV, respectively. The TEM samples were powders spread on Cu grids covered by carbon films. The melting temperatures of the phases were determined by differential thermal analysis (DTA) at rates of 5–20 °C/min.

3. Results and discussion

3.1. Intermediate phases

All of the above-mentioned temperature and compositional ranges include the binary Al–Ru intermediate phases

* Corresponding author at: Institut für Festkörperforschung, Forschungszentrum Jülich, D-52425 Jülich, Germany. Tel.: +49 2461 614693; fax: +49 2461 616444.
E-mail address: d.pavlyuchkov@fz-juelich.de (D. Pavlyuchkov).

0925-8388/$ – see front matter © 2007 Elsevier B.V. All rights reserved.
doi:10.1016/j.jallcom.2007.09.095

Table 1
Crystallographic data of the periodic Al–Pd–Ru phases mentioned in the text

Phase	S.G. or crystal symmetry	Lattice parameters				For composition
		a (nm)	*b* (nm)	*c* (nm)	*β* (°)	
M-$Al_{13}Ru_4$	*C2/m*	1.5862	0.8188	1.2736	107.77	
Al_2Ru	*Fddd*	0.8012	0.4717	0.8785	–	
β (AlPd)	$Pm\bar{3}m$	0.3036	–	–	–	
C	$Pm\bar{3}$	0.77568(3)	–	–	–	$Al_{74.4}Pd_{7.5}Ru_{18.1}$
C_1	$Im\bar{3}$	1.5532(4)	–	–	–	$Al_{71.7}Pd_{12.0}Ru_{16.3}$
C_2	$Fm\bar{3}$	1.55659(5)	–	–	–	$Al_{67.7}Pd_{19.7}Ru_{12.6}$
F_{40}	*Fcc*	∼3.97	–	–	–	
ε	*Orthor.*	∼2.35	∼1.68	Var.*		

The lattice parameters are given for the compositions indicated.
* The structural variants designated ε_6 and ε_{28}, typical of binary Al–Pd, have $c \approx 1.23$ nm and $c \approx 5.70$ nm, respectively [10], in regular ε_{16} $c \approx 3.24$ nm.

M-$Al_{13}Ru_4$ and Al_2Ru (see Table 1). Of the Al–Pd binary phases, only AlPd is solid above 1000 °C. Isostructural congruent AlPd and AlRu (probably) form a continuous range of solid solutions naturally separating the high-Al region of Al–Pd–Ru. This has not yet been studied due to difficulties in the equilibration of the relevant samples. For this reason, the range around the Al_3Ru_2 phase was also excluded from our study. The M-$Al_{13}Ru_4$, and Al_2Ru phases were found to dissolve only a little of Pd: $Al_{13}Ru_4 < 2.5$ at.%, Al_2Ru up to 1 at.%.

The Al-Pd *ε*-phases are solid below 790 °C [10], but with the increase of the Ru concentration this temperature increases reaching 1030 °C at ∼15.5 at.% Ru. Therefore, this phase already appeared in the 1000 °C isothermal section (see below) in a ternary range separated from the Al–Pd terminal. The continuity of this range was confirmed by investigation of intermediate alloys at lower temperatures and by diffraction examinations. Similar to the crystal structures typical of other Al–Pd–TM alloy systems [1], the structures observed in Al–Pd and ternary alloys belonging to the *ε*-range exhibited variations. The lattice parameters of the phases of the ε_l-family $a = 2.35$ and $b = 1.68$ nm were essentially the same, while the *c* parameters are ≈1.23, 3.24, 4.49, 5.70, . . . nm. In the following we designate them ε_6, ε_{16}, ε_{22}, $\varepsilon_{28,\ldots}$, respectively, where the index is the number *l* of the strong (0 0 *l*) reflection corresponding to the interplanar spacing of about 0.2 nm. Apart from the four specific structural variants ε_6, ε_{16}, ε_{22} and ε_{28}, irregular structures were observed in these continuous ranges. The geometry of the *ε*-phases has been described in more detail in [12,13].

In Al–Pd, the high-temperature ε_6 and ε_{28} variants were formed around ∼75 at.% Al. Although two binary structures were observed in Al–Pd, *ε* is presented as one range in the ternary

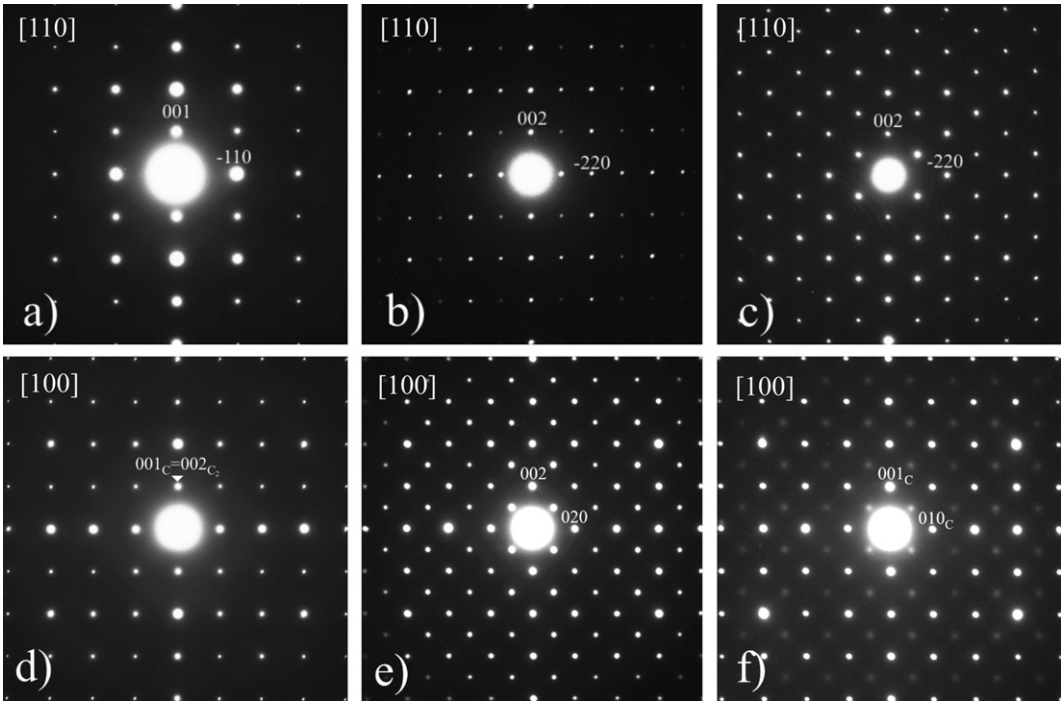

Fig. 1. Electron diffraction patterns of the C-phase (a, d), C_1-phase (b, e) and C_2-phase (c, d). The electron diffraction patterns in (f) were obtained from a sample of the $Al_{71.0}Pd_{12.5}Ru_{16.5}$ composition equilibrated at 1000 °C and subsequently water quenched. The patterns in (a–c) correspond to Z.A. = [1 1 0], in (d–f) to Z.A. = [1 0 0].

phase diagrams. According to [10], the ε_{28} structure is formed at lower Al concentrations than ε_6. More recently [14], the ε_6 structure was also revealed after much longer annealing times at the compositions associated with ε_{28} in [10], but at lower temperatures. This is more consistent with the continuity of the ε-ranges observed in ternary systems, but points to a need for an additional refinement of the Al–Pd phase diagram. The structures in the ε-range of Al-Pd-Ru will be described in more detail elsewhere.

Three cubic phases isostructural to the Al–Pd–Fe C, C_1 and C_2 phases were revealed in Al–Pd–Ru. They are designated hereafter in the same way. The electron diffraction patterns of these phases are compared in Fig. 1.

The primitive cubic C-phase ($Pm\bar{3}$) was formed in a compositional range between about $\sim Al_{73.0}Pd_{5.0}Ru_{22.0}$ and $Al_{70.5}Pd_{15.0}Ru_{14.5}$. Its powder XRD pattern is shown in Fig. 2a and the powder diffraction data in Table 2. The refined lattice parameter was $a = 0.77568(3)$ nm for the $Al_{74.4}Pd_{7.5}Ru_{18.1}$ composition. The highest melting temperature of C was 1326 °C.

The body-centered cubic C_1-phase ($Im\bar{3}$) was formed below 1000 °C. The single-phase sample of C_1 has not yet been obtained. The refinement of its lattice parameter was done using the diffraction data from a sample annealed at 900 °C containing some Al_2Ru (see Table 3). The value of $a = 1.5532(4)$ nm was obtained for $Al_{71.0}Pd_{12.5}Ru_{16.5}$. The lattice parameter of the C_1-phase is twice as large as that of the C-phase.

The diffraction reflections typical of the C_1-phase were also observed in samples of $Al_{71.0}Pd_{12.5}Ru_{16.5}$ and close compositions annealed at 1000 °C, but this was associated with transformations occurring during cooling. Indeed, while the intensities of these reflections in air-cooled samples, in addition to those of the C-phase, were as in the material annealed at 900 °C (Fig. 1e), in water-quenched samples of the same composition they were significantly weaker (Fig. 1f). Even by very sharp quenching the formation of the C_1-phase could not be suppressed. From the quenching experiments we conclude that the above-mentioned compositional range belongs at 1000 °C to the C-phase (see below).

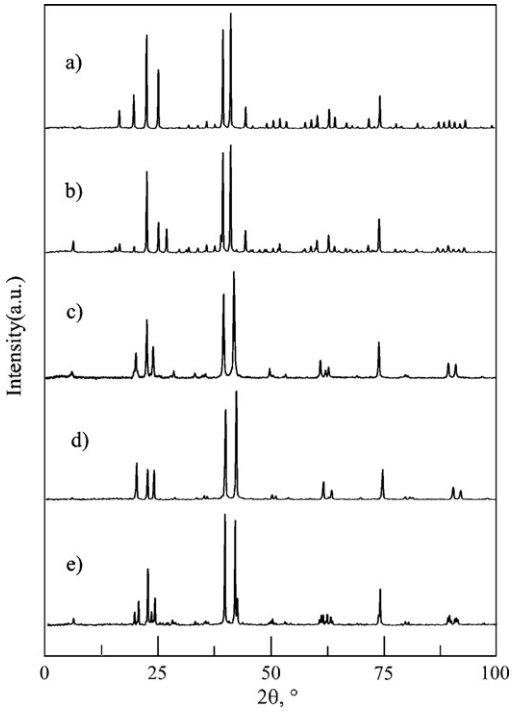

Fig. 2. Powder XRD patterns (Cu $K_{\alpha 1}$ radiation) of the: (a) C-phase, (b) C_2-phase, (c) Al–Pd–Ru I-phase, (d) I-phase of $Al_{64.3}Cu_{23.3}Ru_{12.4}$ [16] and (e) F_{40}-phase.

Table 2
Powder XRD data of the C-phase of the $Al_{74.4}Pd_{7.5}Ru_{18.1}$ composition ($a = 0.77568(3)$ nm, $V = 0.46672(3)$ nm^3)

No.	h	k	l	d^{obs}	d^{calc}	I/I_0^{obs}
1	1	0	0	0.77742	0.77568	2
2	1	1	1	0.44795	0.44784	16
3	2	0	0	0.38782	0.38784	30
4	2	1	0	0.34706	0.34690	83
5	2	1	1	0.31667	0.31667	52
6	2	2	0	0.27397	0.27425	1
7	3	0	0	0.25881	0.25856	3
8	3	1	0	0.24531	0.24529	3
9	3	1	1	0.23382	0.23388	6
10	2	2	2	0.22393	0.22392	4
11	3	2	0	0.21516	0.21514	87
12	3	2	1	0.20729	0.20731	100
13	4	0	0	0.19387	0.19392	19
14	4	1	0	0.18819	0.18813	2
15	3	3	0	0.18260	0.18283	1
16	3	3	1	0.17791	0.17795	4
17	4	2	0	0.17345	0.17345	7
18	4	2	1	0.16926	0.16927	8
19	3	3	2	0.16537	0.16538	6
20	5	0	0	0.15514	0.15514	5
21	5	1	0	0.15211	0.15212	7
22	5	1	1	0.14928	0.14928	11
23	5	2	0	0.14406	0.14404	16
24	5	2	1	0.14164	0.14162	9
25	4	4	0	0.13712	0.13712	5
26	4	4	1	0.13501	0.13503	3
27	5	3	0	0.13305	0.13303	1
28	6	0	0	0.12930	0.12928	9
29	6	1	1	0.12583	0.12583	29
30	6	2	0	0.12273	0.12265	1
31	5	4	0	0.12115	0.12114	4
32	5	4	1	0.11969	0.11969	2
33	6	3	0	0.11563	0.11563	4
34	6	3	1	0.11436	0.11437	2
35	7	0	0	0.11082	0.11081	6
36	7	1	0	0.10970	0.10970	6
37	7	1	1	0.10861	0.10862	7
38	6	4	0	0.10755	0.10757	6
39	7	2	0	0.10654	0.10655	4
40	7	2	1	0.10555	0.10556	7

The face-centered cubic C_2-phase ($Fm\bar{3}$) was formed in a wide compositional range between about $\sim Al_{69.5}Pd_{14.5}Ru_{16}$ and $Al_{68}Pd_{23}Ru_9$. Its powder XRD pattern (Fig. 2b, Table 4) was indexed using $a = 1.55659(5)$ nm for the $Al_{67.7}Pd_{19.7}Ru_{12.6}$ composition. The highest melting temperature of C_2 was 1184 °C.

Although quantitatively the compositional regions of the Al–Pd–Ru C, C_1 and C_2 phases were somewhat different from

those in Al–Pd–Fe [3], the "chain" arrangement of these regions and their sequence were the same.

On the other hand, the existence of the cubic $Al_{68}Pd_{20}Ru_{12}$ phase reported in [6] was not confirmed. In contrast to the diffraction patterns of C_1 and C_2, this phase reported to have essentially the same lattice parameter $a = 1.5540$ nm as C_1 and C_2 but a *different* space group $P23$, would not exhibit regular extinctions. Such electron diffraction patterns were not observed in any of our samples. The powder XRD pattern calculated from the crystal data of [6] was similar to our experimental pattern obtained from the sample of the $Al_{70}Pd_{17}Ru_{13}$ composition annealed at 900 °C and containing a mixture of the C_1 and C_2 phases. The sample studied in [6] by single-crystal X-ray diffractometry probably solidified primarily to the C_2-phase, but partially transformed to the C_1-phase during cooling, similarly to that observed in the low-Ru C-phase (see above). Both cubic structures were perfectly oriented producing a diffraction pattern similar to that produced by a single phase. Such coherent precipitation had been previously observed in the Al-Pd-Fe alloy system, where similar C_1 and C_2 phases were formed [2,15]. In fact, the authors of [6] observed some regular extinctions, but ignored this information. A more detailed explanation of this phenomenon and its interpretation will be published elsewhere.

The stability of the ternary icosahedral quasicrystalline phase (I-phase) was confirmed by prolonged annealing at 1000 °C. The I-phase was formed in a compositional range between $\sim Al_{72.5}Pd_{13}Ru_{14.5}$ and $Al_{70.0}Pd_{19.5}Ru_{10.5}$. Its highest melting temperature was 1080 °C. It is isostructural to other stable I-phases in ternary alloy systems of Al with transition metals (see [1] for references). For example, the powder XRD pattern of the Al–Pd–Ru I-phase (Fig. 2c) was very similar to that of the Al–Cu–Ru I-phase published in [16] (see Fig. 2d for the $Al_{64.3}Cu_{23.3}Ru_{12.4}$ composition).

A face-centered cubic phase with $a \approx 3.96$ nm was revealed close to the above-mentioned range of the I-phase around composition $Al_{72.5}Pd_{13}Ru_{14}$. In the following, it is designated F_{40}-phase. The typical electron diffraction patterns are shown in Fig. 3a–c. Its XRD pattern (Fig. 2e) exhibited a close structural relation to the I-phase. Due to such a large unit cell, reliable indexation of the powder XRD pattern is difficult and not yet complete.

Due to the similarity of their powder XRD patterns, the coexistence of the I and F_{40} phases cannot be detected by X-ray diffractometry. We also used SEM/EDX and could not detect any compositional gaps between the assumed single-phase regions.

Table 3
Powder XRD data of the C_1-phase of the $Al_{71.3}Pd_{12.5}Ru_{16.2}$ composition ($a = 1.5532(4)$ nm, $V = 3.7467(15)$ nm^3)

No.	h	k	l	d^{obs}	d^{calc}	I/I_0^{obs}
1	1	1	0	1.10164	1.09825	9
2	2	2	2	0.44810	0.44836	7
3	4	0	0	0.38858	0.38829	11
4	4	2	0	0.34724	0.34730	52
5	4	2	2	0.31712	0.31704	26
6	4	4	0	0.27467	0.27456	3
7	6	0	0	0.25849	0.25886	3
8	6	2	0	0.24538	0.24558	2
9	6	2	2	0.23406	0.23415	5
10	4	6	0	0.21533	0.21538	57
11	4	6	2	0.20757	0.20755	100
12	8	0	0	0.19412	0.19414	14
13	8	4	0	0.17373	0.17365	4
14	8	4	2	0.16955	0.16946	5
15	6	6	4	0.16564	0.16557	2
16	10	0	0	0.15529	0.15532	3
17	10	2	0	0.15228	0.15230	5
18	10	2	2	0.14945	0.14945	9
19	10	4	0	0.14423	0.14421	12
20	10	4	2	0.14180	0.14178	5
21	8	8	0	0.13729	0.13728	3
22	12	0	0	0.12935	0.12943	5
23	12	2	2	0.12601	0.12598	21

Table 4
Powder XRD data of the C_2-phase of the $Al_{67.7}Pd_{19.7}Ru_{12.6}$ composition ($a = 1.55659(5)$ nm, $V = 3.77155(21)$ nm^3)

No.	h	k	l	d^{obs}	d^{calc}	I/I_0^{obs}
1	1	1	1	0.89868	0.89870	11
2	3	1	1	0.47002	0.46933	5
3	2	2	2	0.44956	0.44935	8
4	4	0	0	0.38908	0.38915	6
5	4	2	0	0.34825	0.34806	76
6	4	2	2	0.31792	0.31774	28
7	5	1	1	0.29976	0.29957	22
8	4	4	0	0.27530	0.27517	3
9	5	3	1	0.26340	0.26311	3
10	6	0	0	0.25966	0.25943	5
11	6	2	0	0.24624	0.24612	4
12	6	2	2	0.23469	0.23466	7
13	4	4	4	0.22473	0.22467	6
14	7	1	1	0.21794	0.21797	16
15	6	4	0	0.21589	0.21586	92
16	6	4	2	0.20801	0.20801	100
17	7	3	1	0.20263	0.20265	2
18	8	0	0	0.19459	0.19457	20
19	8	2	0	0.18874	0.18876	3
20	6	6	0	0.18349	0.18345	3
21	7	5	1	0.17979	0.17974	3
22	6	6	2	0.17854	0.17855	3
23	8	4	0	0.17405	0.17403	4
24	8	4	2	0.16983	0.16984	8
25	10	0	0	0.15566	0.15566	4
26	10	2	0	0.15263	0.15264	6
27	9	5	1	0.15046	0.15048	4
28	10	2	2	0.14978	0.14978	11
29	10	4	0	0.14454	0.14453	16
30	10	4	2	0.14211	0.14210	6
31	8	8	0	0.13760	0.13758	4
32	11	3	1	0.13603	0.13600	3
33	10	6	0	0.13347	0.13348	2
34	12	0	0	0.12973	0.12972	7
35	12	2	2	0.12626	0.12626	31
36	10	8	0	0.12155	0.12155	3
37	13	1	1	0.11901	0.11904	2
38	12	6	0	0.11602	0.11602	3
39	14	0	0	0.11120	0.11118	4
40	14	2	0	0.11004	0.11007	3
41	14	2	2	0.10898	0.10898	6
42	12	8	0	0.10791	0.10793	3
43	14	4	0	0.10690	0.10691	3
44	14	4	2	0.10589	0.10591	4

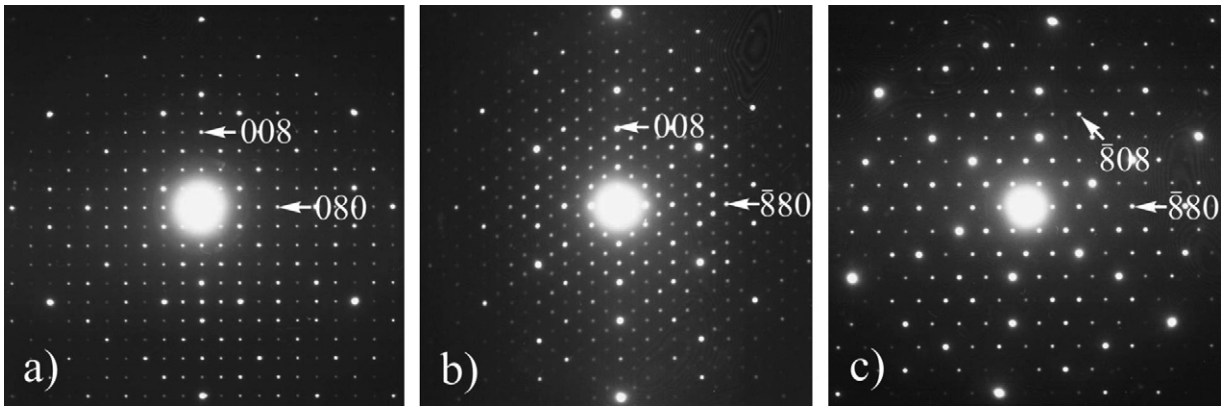

Fig. 3. Electron diffraction patterns of the F_{40}-phase along the [1 0 0], [1 1 0] and [1 1 1] zone axes.

Therefore, in the following we will include this cubic structure in one region designated "I"-region. It is worth noting that in Al–Cu–Fe [17] and Al–Pd–Mn [18], a number of complex periodic phases were also observed at compositions very close to those of the icosahedral phase. The compositional range of the Al–Pd–Ru I-phase at 1000 °C had only shifted slightly from those in Al–Pd–Mn [19] and Al–Pd–Re [15]. Detailed description of the I-region requires additional study.

3.2. Isothermal sections

The partial isothermal section at 1100 °C is presented in Fig. 4. In the studied compositional range the Al_2Ru and $Al_{13}Ru_4$ were solid at this temperature, while the region adjacent to Al–Pd was occupied by the liquid. The limit of Al solubility in the β-phase reached 56 at.% at 3.5 at.% Ru. The $Al_{13}Ru_4$ and Al_2Ru phases extended up to ∼2 and ∼1 at.% Pd correspondingly. The ternary C-phase was formed in a wide range from $\sim Al_{73.0}Pd_{5.0}Ru_{22.0}$ to $Al_{70.5}Pd_{15.0}Ru_{14.5}$. The C_2-phase was also solid at this temperature and occupied a small range around $Al_{68.5}Pd_{18}Ru_{13.5}$. It was in equilibrium with the liquid, C, Al_2Ru and the β-phase.

Several samples were studied at 1050 °C, i.e. slightly above the highest melting temperature of the ε-phases (see Fig. 5). The maximum solubility of Al in β-phase was about 56.9 at.%. The I-phase was already solid at this temperature. It was formed between $\sim Al_{72.5}Pd_{13.5}Ru_{14.0}$ and $Al_{70.5}Pd_{17.5}Ru_{12}$. The C-phase region extended from the $\sim Al_{74.0}Pd_{5.5}Ru_{20.5}$ to $Al_{70.0}Pd_{14}Ru_{16}$ composition. The region of C_2 was significantly wider than at 1100 °C, namely from $\sim Al_{69.5}Pd_{14.5}Ru_{16}$ to $Al_{67.5}Pd_{22.5}Ru_{10}$. The regions of ternary phases were very close to each other, thus several ranges of the three-phase equilibria are narrow. The corresponding tie-lines are shown approximately, based on the results obtained from two-phase samples.

The phase equilibria at 1000 °C are shown in Fig. 6. The limit of Pd solubility in the M-$Al_{13}Ru_4$ phase increased to ∼2.5 at.%, while that of Al_2Ru decreased to ∼0.5 at.%. The limit of the Al solubility in the β-phase was similar to that at 1000 °C. Apart from C, C_2 and I also F_{40} and ε were solid at this temperature. The composition of the C-phase varied in the range from $\sim Al_{74.0}Pd_{5.5}Ru_{20.5}$ to $Al_{71.5}Pd_{14.5}Ru_{14.0}$. The C_2-phase had a compositional range between $\sim Al_{70.5}Pd_{15.0}Ru_{14.5}$ to $Al_{68}Pd_{23}Ru_9$. I-region was formed in the compositional range between $\sim Al_{72.5}Pd_{13}Ru_{14.5}$ and $Al_{70.0}Pd_{19.5}Ru_{10.5}$. The F_{40}-

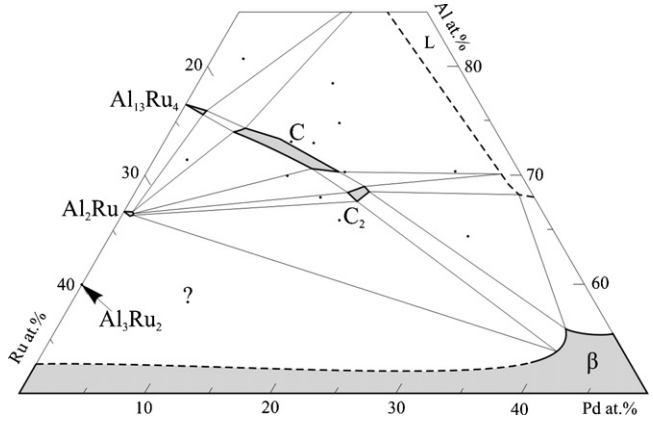

Fig. 4. Partial isothermal section of Al–Pd–Ru at 1100 °C. The compositions of the studied alloys are marked by dots, the provisional tie-lines are shown by dotted lines, suggested regions of homogeneity of the phases by broken lines. The liquid is designated L, M-$Al_{13}Ru_4$ is M. The region marked by (?) was not studied.

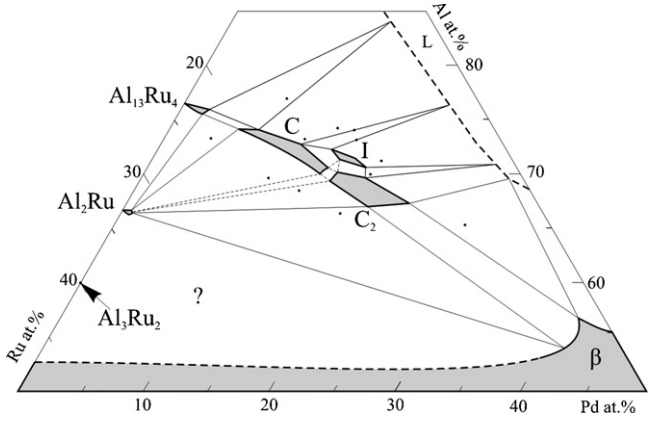

Fig. 5. Partial isothermal section of Al–Pd–Ru at 1050 °C. The compositions of the studied alloys are marked by dots, the provisional tie-lines are shown by dotted lines, suggested regions of homogeneity of the phases by broken lines. The liquid is designated L, M-$Al_{13}Ru_4$ is M. The region marked by (?) was not studied.

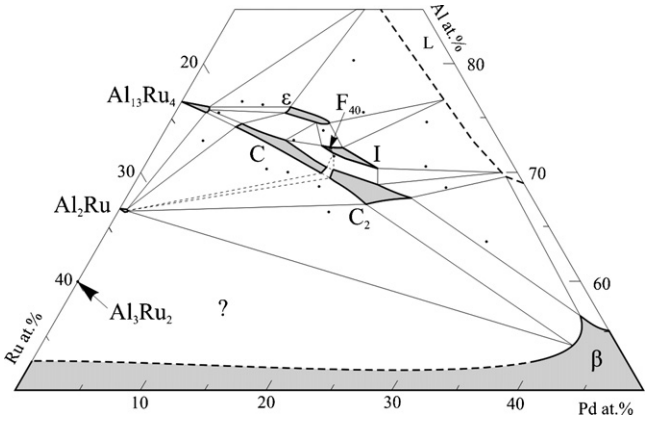

Fig. 6. Partial isothermal section of Al–Pd–Ru at 1000 °C. The compositions of the studied alloys are marked by dots, the provisional tie-lines are shown by dotted lines, suggested regions of homogeneity of the phases by broken lines. The liquid is designated L, M-$Al_{13}Ru_4$ is M. The region marked by (?) was not studied.

phase existed around the high-Ru limit of the I-region. The ε-range extended from ~$Al_{76.0}Pd_{8.5}Ru_{15.5}$ to $Al_{75.0}Pd_{12}Ru_{13}$. The three-phase equilibria liquid-ε-"I", M-ε-C, ε-C-"I", "I"-C-C_2, C-C_2-Al_2Ru were derived on the basis of the results obtained from two-phase samples.

4. Summary

Al–Pd–Ru belongs to a group of alloy systems that exhibit the formation of quasicrystals and related complex periodic intermetallics. The stability of the ternary quasiperiodic icosahedral phase was confirmed below 1080 °C. A complex cubic structure with $a \approx 3.96$ nm, closely related to the icosahedral phase, was found to be formed at the high-Ru limit of the icosahedral range which extended between the ~$Al_{72.5}Pd_{13}Ru_{14.5}$ and $Al_{70.0}Pd_{19.5}Ru_{10.5}$ compositions at 1000 °C.

The Al–Pd orthorhombic ε-phases dissolved up to ~15.5 at.% Ru, $Al_{13}Ru_4$ <2.5 at.% Pd and Al_2Ru up to 1 at.% Pd. Between 66 and 75 at.% Al, three cubic phases: C ($Pm\bar{3}$, $a = 0.7757$ nm), C_1 ($Im\bar{3}$, $a = 1.5532$ nm) and C_2 ($Fm\bar{3}$, $a = 1.5566$ nm) were revealed. Although quantitatively the compositional regions of the Al–Pd–Ru C, C_1 and C_2 phases were somewhat different from those in Al-Pd-Fe, the "chain" arrangement of these regions and their sequence were the same. On the other hand, the existence of the cubic $Al_{68}Pd_{20}Ru_{12}$ phase ($P23$; $a = 1.5540$ nm) reported in the literature was not confirmed.

Partial isothermal sections of the Al–Pd–Ru phase diagram at 1000, 1050 and 1100 °C were determined.

Acknowledgements

We thank W. Reichert and M. Schmidt for technical contributions and S. Balanetskyy, M. Yurechko and S. Mi for helpful discussions.

References

[1] B. Grushko, T. Velikanova, CALPHAD 31 (2007) 217.
[2] S. Balanetskyy, B. Grushko, E. Kowalska-Strzęciwilk, T.Ya. Velikanova, K. Urban, J. Alloys Compd. 364 (2004) 166.
[3] S. Balanetskyy, B. Grushko, T. Velikanova, K. Urban, J. Alloys Compd. 368 (2004) 169;
S. Balanetskyy, B. Grushko, T. Velikanova, K. Urban, J. Alloys Compd. 376 (2004) 158.
[4] B. Przepiórzyński, B. Grushko, M. Surowiec, Intermetallics 14 (2006) 498.
[5] S. Mi, B. Grushko, C. Dong, K. Urban, J. Alloys Compd. 351 (2002) L1;
S. Mi, B. Grushko, C. Dong, K. Urban, J. Alloys Compd. 359 (2003) 193.
[6] S. Mahne, W. Steurer, Z. Kristall. 211 (1996) 17.
[7] K. Sugiyama, K. Hiraga, K. Saito, Mater. Sci. Eng. A294–296 (2000) 345.
[8] T. Shibuya, T. Asao, M. Tamura, R. Tamura, S. Takeuchi, Mater. Sci. Eng. A294–296 (2000) 61.
[9] T. Asao, R. Tamura, S. Takeuchi, Phil. Mag. Lett. (2002) 217.
[10] M. Yurechko, A. Fattah, T. Velikanova, B. Grushko, J. Alloys Compd. 329 (2001) 173.
[11] S. Mi, S. Balanetskyy, B. Grushko, Intermetallics 11 (2003) 643.
[12] M. Yurechko, B. Grushko, T.Ya. Velikanova, K. Urban, in: T.Ya. Velikanova (Ed.), Phase Diagrams in Materials Science, MSIT, Stuttgart, 2004, p. 92, http://www.matport.com/publishing/pdms/index.shtml.
[13] S. Balanetskyy, B. Grushko, T. Velikanova, Z. Kristal. 219 (2004) 548.
[14] S. Balanetskyy, B. Grushko, unpublished report.
[15] S.O. Balanetskii (Balanetskyy), B. Grushko, K. Urban, T.Ya. Velikanova, Powder Metall. Metal Ceram. 43 (2004) 396.
[16] S. Mi, B. Grushko, Intermetallics 12 (2004) 425.
[17] M. Quiquandon, A. Quivy, J. Devaud, F. Faudot, S. Lefebvre, M. Bessiere, Y. Calvayrac, J. Phys.: Condens. Matter 8 (1996) 2487.
[18] H.L. Li, K.H. Kuo, Phil. Mag. Lett. 70 (1994) 55.
[19] B. Grushko, Mater. Sci. Eng. A294–296 (2000) 45.